*Materials Transactions*, Vol. 55, No. 11 (2014) pp. 1770 to 1776

**EXPRESS REGULAR ARTICLE**

# Numerical Study on Effective Thermal Conductivity of Radial Nanowire Heterostructures with MWCNT Core

Joo Hyun Moon[1], Jeongmin Lee[1], Jooheon Kim[2] and Seong Hyuk Lee[1,*]

[1]*School of Mechanical Engineering, Chung-Ang University, 221 Heuksuk-Dong, Dongjak-Gu, Seoul 156-756, Korea*
[2]*School of Chemical Engineering and Materials Science, Chung-Ang University, 221 Heuksuk-Dong, Dongjak-Gu, Seoul 156-756, Korea*

The present study aims to investigate numerically the effective thermal conductivity for different radial nanowire heterostructures (RNWHSs), such as core–shell, tubular–shell, and core–shell–shell types, which are used for resolving thermal dissipation problem. The influence of core radius and shell thickness on the effective thermal conductivity was examined by using the boundary/interfacial scattering (BS) method derived from the Casimir theory. It was found that the effective thermal conductivity of the RNWHSs was smaller than the bulk thermal conductivity of multi-walled carbon nanotubes (MWCNTs) because of the diffusive interfacial scattering effect. When the shell thickness was much thinner than the core radius, the thermal conductivity of the core MWCNT was relatively higher than that of the shell material. Comparing MWCNT/$Al_2O_3$ and MWCNT/$SiO_2$ core–shell RNWHSs, the effective thermal conductivities were similar when the core radius was greater than 100 nm or the core porosity was above 0.4, owing to the effect of MWCNT bulk thermal conductivity. Besides, the effective thermal conductivity of the tubular–shell RNWHS with the same cross-sectional area was always lower than that of the core–shell RWNHSs because of additional interfacial scattering at the pores inside the tubular-shell RNWHSs. When the $Al_2O_3$ thickness in the core–shell–shell RNWHS of MWCNT/$Al_2O_3$/W was less than 135 nm at a fixed MWCNT radius of 100 nm, the effective thermal conductivity increased with core porosity. When the $Al_2O_3$ thickness was 1.0 nm, the effective thermal conductivity rapidly decreased with the increase in porosity.
[doi:10.2320/matertrans.M2014191]

(Received May 19, 2014; Accepted September 1, 2014; Published October 18, 2014)

***Keywords:*** *Casimir theory, effective thermal conductivity, multi-walled carbon nanotube (MWCNT), phonon mean free path, radial nanowire heterostructure (RNWHS)*

## 1. Introduction

For practical energy conversion applications such as electronic and opto-electronic devices, controlling the thermal conductivity is crucial for improving the safety and durability of these devices through robust heat transfer. For example, thermally conductive polymer composites have been widely used as thermal interfacial materials to dissipate heat and prevent excessive electrical charge.[1–5] Polymer resins have been widely used to make the thermally conductive composites used in many electronic packaging applications.

To enhance the thermal conductivity, high-aspect ratio and highly conductive materials such as multi-walled carbon nanotubes (MWCNTs) can be used as fillers in polymer resins as compared to ceramic nanoparticle fillers because the bulk thermal conductivity of MWCNTs is one of the highest.[6,7] Because MWCNTs have very high thermal conductivity and thermoelectric power, they would be splendid candidates for fabricating radial nanowire heterostructures (RNWHSs) on MWCNT cores, with a dielectric shell layers.[8–13] Among the previous attempts to make RNWHSs, Im and Kim[3,14] fabricated RNWHSs using a MWCNT core on which an $Al(OH)_3$ shell was coated for electrical insulation. They measured the thermal conductivity and diffusivity of the conductive composites, and suggested an empirical correlation for thermal diffusivity. Moreover, they showed that the thermal conductivity of the fillers increased with the increase in MWCNT porosity. Zhang *et al.*[15] modified the surfaces of MWCNTs with an insulated inorganic alumina compound layer to improve the homogenous dispersion of the MWCNTs in the solvent or the polyimide matrix. The transparency and thermal conductivity of the modified polymer composites were significantly improved with electric insulation. Cui *et al.*[16] synthesized silica-coated ($SiO_2$) MWCNT-core RNWHSs by using the sol–gel method to maintain the high thermal conductivity. The MWCNT–$SiO_2$ RNWHSs in a soft epoxy matrix improved the thermal conductivity while retaining the high electrical resistivity of the composites even though MWCNTs are a good electrically conductive material.[16]

Herrmann *et al.*[17] coated multi-shells on MWCNT cores by using the atomic layer deposition method (ALD) in order to make dielectric and thermally conductive materials. They fabricated multi-shell RWNHSs consisting of $Al_2O_3$, and W shell layers and visualized them by transmission electronic microscopy (TEM).[17] These coating layers on MWCNTs can be applied as electrical insulation in coaxial nanotube cables.

There have been a number of previous studies on the feasibility of measuring the thermal and electrical conductivity of composites using bundles of RNWHSs. In fact, it is very difficult to measure the thermal and electrical conductivity of individual RNWHSs directly. Hence, many theoretical and numerical attempts have been reported for the calculation of RNWHS thermal conductivity with respect to the properties and geometrical shape of these structures, such as their wire radius and porosity.[5,18–21] Yang *et al.*[20,21] used the phonon Boltzmann transport equation to examine the effect of geometry on the thermal conductivity of core–shell and tubular–shell nanowires. They also used the effective medium theory related to the thermal boundary resistance and the Fourier heat conduction law to calculate the effective thermal conductivity of core–shell and tubular–shell Si/Ge RNWHSs with respect to surface diffusion/specular conditions.[20,21] Prasher[22] reported an analytical solution of the

*Corresponding author, E-mail: shlee89@cau.ac.kr

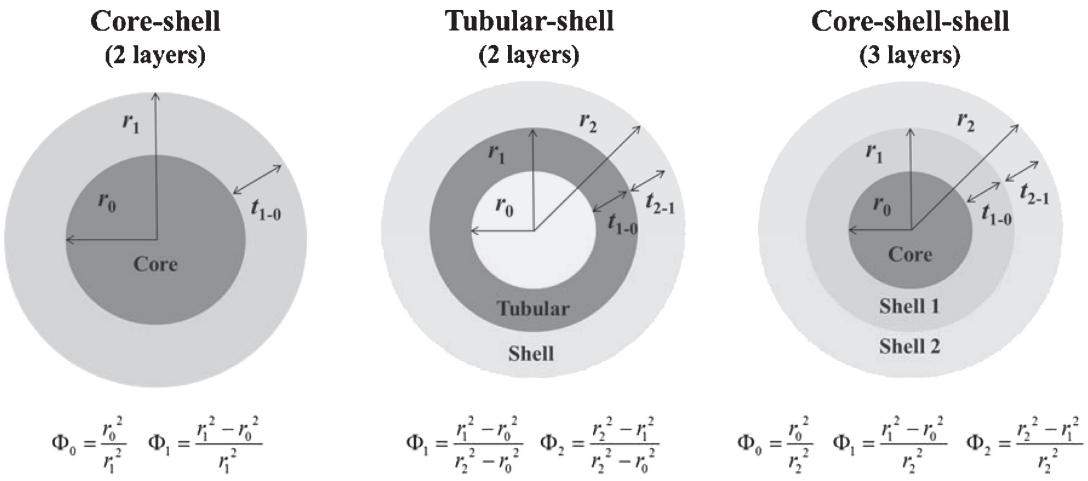


Fig. 1 Cross sections of various types of RNWHSs used in this study, showing their radii, thicknesses, and porosities.

phonon Boltzmann transport equation for tubular– and core–shell RNWHS types, which showed that the thermal conductivities of these structures were significantly lower than the bulk thermal conductivity of MWCNT.

Lü[23] suggested the theoretical model to investigate the effect of size on the thermal conductivity of RNWHSs by considering the boundary scattering effects at the internal and external interfaces using some analytical solutions.[18,23,24] In his work, the Boltzmann transport equation was first used to calculate partially specular RNWHSs by modifying Prasher's analytical solution.[19,22,23] Also, on the basis of Matthiessen rule and Casimir theory, the effective thermal conductivity was estimated by using a simple analytical solution that included the interfacial scattering phonon mean free path (MFP).[18] Moreover, he introduced simple analytical models for estimating the effective thermal conductivity of square nanopores of periodically arranged Si by referring to Prasher's model.[22,24]

Even though some efforts have been made, there is still a lack of numerical studies for estimating the effective thermal conductivity of a single RNWHS with an MWCNT core coated with various shell materials. It is thus obvious that the thermal conductivity of a single RNWHS as a unit concept should be understood in order to effectively design a conductive polymer that includes an MWCNT core. On the basis of the boundary/interfacial scattering (BS) theory, the present study aims to numerically investigate the effective thermal conductivity of a single RNWHS with an MWCNT core coated with dielectric materials. Core–shell, tubular–shell, and core–shell–shell RNWHS types, illustrated in Fig. 1, are investigated in order to examine the influence of core radius and shell thickness on the effective thermal conductivity.

## 2. Mathematical Representation

Figure 2 illustrates an RNWHS considered for the present study and shows that the phonon undergoes the scattering events of a totally diffuse scattering case, which can be distinguished by the critical angle $\theta_C$ on the cross section.[18] When $\theta < \theta_C$, phonons only hit the external interfaces, such as projected paths $AB$ and $AC$ in Fig. 2. On the other hand, phonons only hit the internal interface along the projected path $AE$ related to $\theta_C$.[18] The effective longitudinal thermal conductivity of an RNWHS with $n$ layers can be evaluated as follows:

$$K_{\mathrm{RNWHS}} = \sum_{j=0}^{n} k_j \Phi_j, \tag{1}$$

where $j = 0$ for the core layer and $j > 0$ for the $j$th shell layer along the radial direction. The symbol $\Phi$ denotes the area porosity of the RNWHS, which can be expressed in terms of the radii. As shown in Fig. 1, $\Phi_0 = {r_0}^2/{r_1}^2$ and $\Phi_1 = ({r_1}^2 - {r_0}^2)/{r_1}^2$ for the core–shell type, $\Phi_1 = ({r_1}^2 - {r_0}^2)/({r_2}^2 - {r_0}^2)$ and $\Phi_2 = ({r_2}^2 - {r_1}^2)/({r_2}^2 - {r_0}^2)$ for the tubular–shell type, and $\Phi_0 = {r_0}^2/{r_2}^2$, $\Phi_1 = ({r_1}^2 - {r_0}^2)/{r_2}^2$, and $\Phi_2 = ({r_2}^2 - {r_1}^2)/{r_2}^2$ for the core–shell–shell type. The thermal conductivity of air in the pores of the tubular–shell type can be ignored because its value is typically 0.03 $\mathrm{W\,m^{-1}\,K^{-1}}$ at 300 K,[18] which is significantly smaller than that of MWCNTs. By using Matthiessen rule, the MWCNT thermal conductivity can be described as $k_{\mathrm{bulk}}[1 + \Lambda_{\mathrm{bulk}}/\Lambda_{\mathrm{BS}}]^{-1}$, where $k_{\mathrm{bulk}}$ and $\Lambda_{\mathrm{bulk}}$ are the bulk thermal conductivity and the MFP, respectively, as listed in Table 1. The boundary/interfacial scattering MFP can be expressed as

$$\Lambda_{\mathrm{BS}} = \frac{3}{4\pi} \frac{\iint (z_{\mathrm{R}} \cos\alpha_1 \cos\alpha_2 / R^2) \mathrm{d}S_1\, \mathrm{d}S_2}{\int \mathrm{d}S_1}, \tag{2}$$

Table 1 Bulk thermal conductivity and mean free path for each material at 300 K.

| Name | Bulk thermal conductivity ($\mathrm{W\,m^{-1}\,K^{-1}}$) | Bulk mean free path (nm) |
|---|---|---|
| Si | 150[20] | 268.2[20] |
| Ge | 60[20] | 198.6[20] |
| MWCNT | 3000[8] | 500[8] |
| $SiO_2$ | 1.4[26] | 0.8[27] |
| $Al_2O_3$ | 30[28] | 95.1[29] |
| W | 174[30] | 10[31] |

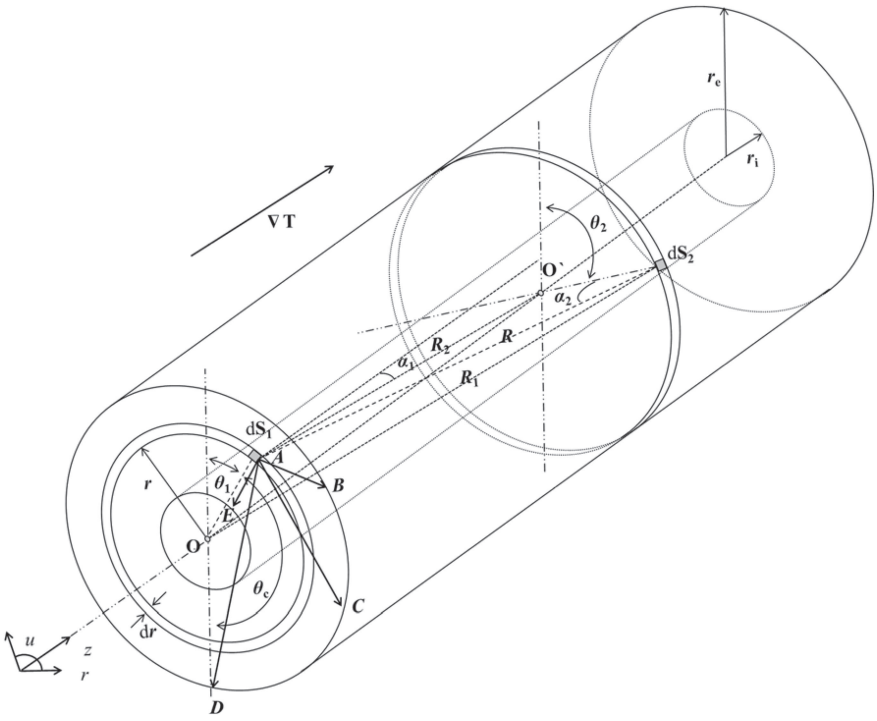


Fig. 2 A schematic diagram of a RNWHS.

where $dS_1$ is an area element on the cross section and $dS_2$ is an area on the interface.[18] $R$ means the module of the vector $\boldsymbol{R}$ connecting $dS_1$ and $dS_2$, and $z_R$ indicates the $z$ component of $R$. The variables $\alpha_1$ and $\alpha_2$ are the angles between the $\boldsymbol{R}$ vector and the normals to $dS_1$ and $dS_2$, respectively. According to Lü,[18] eq. (2) can be simplified as follows:

$$\Lambda_{BS}(r_i, r_e) = \frac{2X(r_e, r_i)}{({r_e}^2 - {r_i}^2)}, \tag{3}$$

$$X(r_e, r_i) = \left(\frac{3}{\pi}\right)\left(-\int_0^{\infty}\int_{r_i}^{r_e}\int_0^{\theta_{C1}} \frac{r_i r z^2 (r_i - r\cos u)}{[r^2 + {r_i}^2 - 2rr_i\cos u + z^2]^2}\,du\,dr\,dz + \int_0^{\infty}\int_{r_i}^{r_e}\int_0^{\theta_C} \frac{r_e r z^2 (r_e - r\cos u)}{[r^2 + {r_e}^2 - 2r_e r\cos u + z^2]^2}\,du\,dr\,dz\right) \tag{4}$$

where $X$ is the size-dependent function, the subscripts i and e mean the internal and external interfaces, respectively, and $\theta_C$ can be defined as $\theta_{C1} + \theta_{C2}$, where $\theta_{C1}$ and $\theta_{C2}$ are expressed as $\cos^{-1}(r_i/r)$ and $\cos^{-1}(r_i/r_e)$, respectively. Moreover, Lü[18] suggested a simple approximate analytical model to simplify $\Lambda_{BS}$ as

$$\Lambda_{BS}(r_i, r_e) \cong 2\,\frac{{r_e}^2 + {r_i}^2 + r_e r_i}{r_e + r_i}\left(1 - \frac{r_i}{r_e}\right). \tag{5}$$

Some literature reported anisotropic characteristics, which indicates thermal conductivity difference between longitudinal and transverse directions.[4,8,25] Similar to the previous study,[14] it is assumed in the present study that the longitudinal direction of thermal conductivity can be expected to be dominant for an RNWHS with $n$th layer. In fact, the RNWHS's length was taken as $10^5$ nm, which was higher than the maximum of radii (~1000 nm). Under this assumption, MWCNT's thermal conductivity of the longitudinal direction would be higher than that of the transverse direction.

## 3. Results and Discussion

For validation, the present study conducted the calculation for predicting the effective thermal conductivity of a Si/Ge core–shell structure under the same conditions used in the literature.[18] Figure 3 compares the predicted thermal conductivity with respect to Si porosity with the estimated thermal conductivity[18] shows quite good agreement (Fig. 3). From the results, the size-dependency of thermal conductivity is clearly observed, in that as the Ge shell thickness increases, rapid enhancement of the thermal conductivity can be achieved. As mentioned above, the approximate model (eq. (5)) is useful for simple estimation of thermal conductivity, but its applicability to the present problem should be evaluated. Hence, the present study compared the numerical results for core–shell (MWCNT/$SiO_2$) and tubular–shell RNWHSs by using two different equations, i.e., eq. (3) and eq. (5). In Fig. 4(a), very good agreement is shown between the analytical and approximation solutions, showing a deviation of less than 2% for all cases. However,

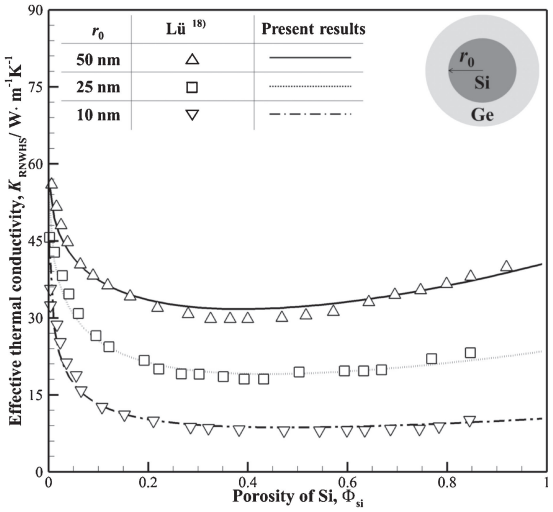


Fig. 3 Effective thermal conductivity comparison between Lü[18)] and this study of a Si/Ge core–shell RNWHS.

Fig. 4(b) clearly shows that the approximation solutions deviate significantly from the analytical solutions for the tubular–shell structure. There is a maximum deviation of approximately 36% for the case in which $r_0 = 1$ nm and $t_{1-0} = 100$ nm. This deviation increases with the increase in porosity of the MWCNT core, showing that numerical accuracy is highly affected by the relative difference in layer thickness and thus layer thickness cannot be ignored numerically. The increase in deviation may be because the size-dependent function $X$ shown in eq. (3) was simply approximated as $(r_e^3 - r_i^3)$ for the tubular nanowire. The core–shell solutions predicted by the approximation and analytical equations are nearly the same under the solid nanowire (SNW) limit ($\Lambda_{BS} \rightarrow 2r_e$).

### 3.1 The effective thermal conductivity of core–shell nanostructures coated with $SiO_2$ and $Al_2O_3$ shells

The present study calculated the effective thermal conductivity of RNWHSs based on their material properties and morphologies, i.e., core/pore radius, shell thickness, and porosity. According to many studies mentioned previously, the bulk thermal conductivity is proportional to $C_v v \Lambda_{bulk}$, where the $C_v$ is the heat capacity per unit volume and the $v$ is the phonon group velocity. As the length of C-C bond is 0.144 nm, lower limit of radius for calculation was above 1 nm[25)] and thicknesses would not above 1 nm.[2,3)] We presented two shell materials for core–shell RNWHSs at a fixed temperature of 300 K: $SiO_2$ and $Al_2O_3$. Their bulk thermal conductivities and mean free paths are lower than those of MWCNTs, as shown in Table 1.

Figure 5(a) shows the effective thermal conductivity of the core–shell (MWCNT/$SiO_2$) RNWHS with respect to MWCNT porosity and core radius. When the core radius was fixed, the increase in the porosity indicated a decrease in the thickness of the coated shell. As the total radius of the RNWHS decreased, the effective thermal conductivity became clearly smaller than the bulk value of the MWCNTs. This is because of the diffuse interfacial scattering effect rather than phonon dispersion.[20)] An MWCNT porosity of unity indicates that there is no shell coated on the core, in

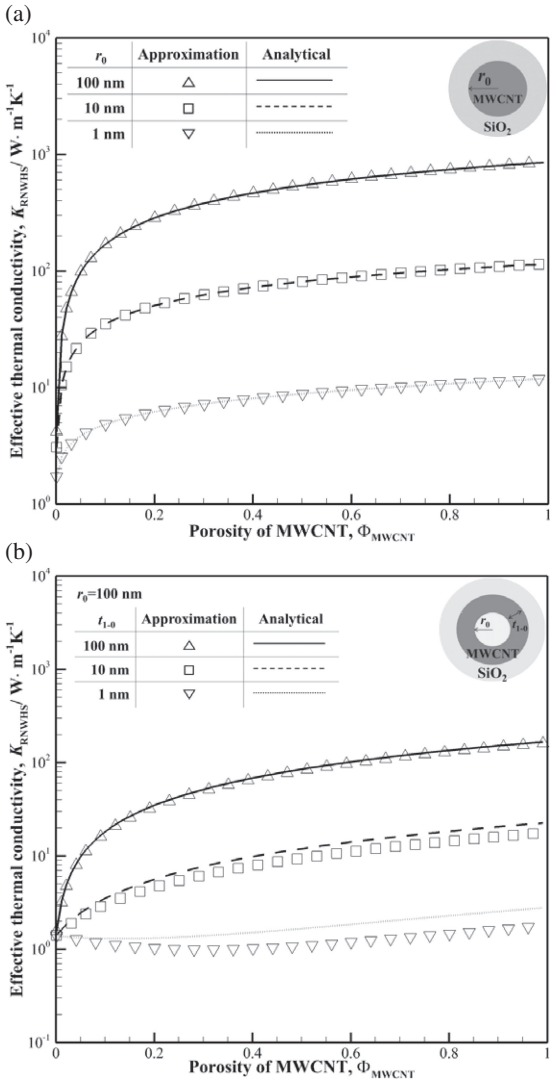


Fig. 4 Comparison of approximation and analytical results.

which case the effective thermal conductivity of the RNWHS is identical to that of the bulk thermal conductivity of the MWCNTs. In addition, the effective thermal conductivity decreased with the decrease in the radius of the MWCNT core, independent of porosity. When the MWCNT radius was very small e.g., $r_0 = 1$ nm, the effective thermal conductivity decreased with increasing MWCNT porosity, i.e., there is a minimum point. Other studies[18,20,21)] have reported that this is because of surface and interfacial scattering due to the relative size difference between the shell thickness and the core radius. The thermal conductivity of $SiO_2$ decreased below the MWCNT thermal conductivity because the MWCNT porosity increased. According to eq. (1), the effective conductivity is associated with the combined thermal conductivities of the core and coated shell, which are considerably affected by the core radius and shell thickness. In particular, there is a minimum thermal conductivity at a certain porosity value. As shown in Fig. 5(a), these different tendencies can be observed the effective thermal conductivity rapidly increases at all radii and porosities. In fact, the bulk thermal conductivity and MFP of an MWCNT are three orders of magnitude higher than those of $SiO_2$. Hence, the effective thermal conductivity

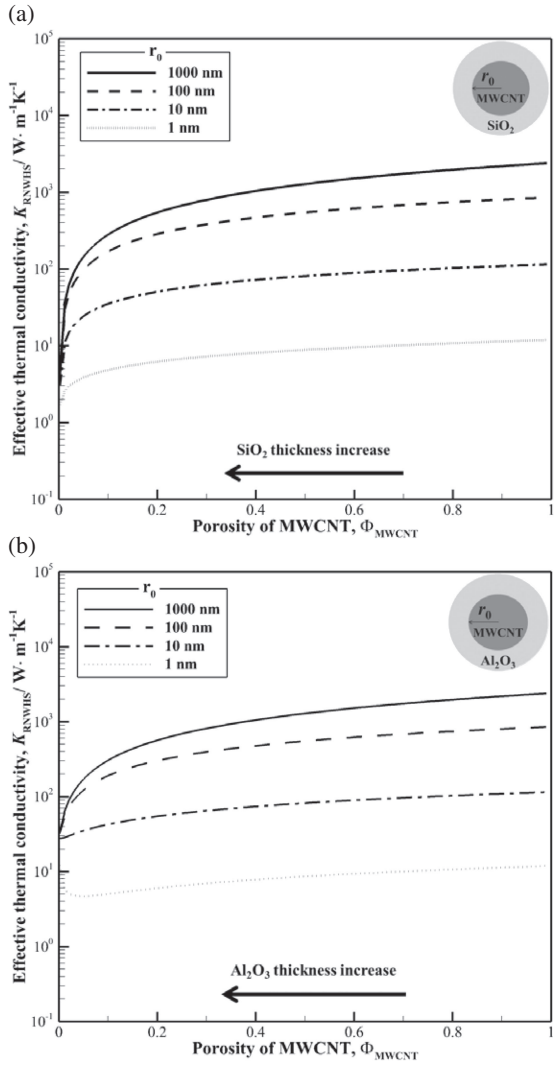


Fig. 5 Effective thermal conductivity of core–shell RNWHSs with respect to MWCNT porosity and core radius for.

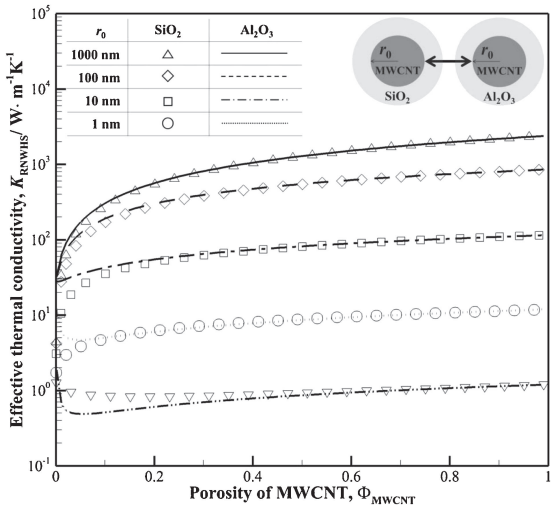


Fig. 6 Effective thermal conductivity comparison between MWCNT/$SiO_2$ and MWCNT/$Al_2O_3$ RNWHSs.

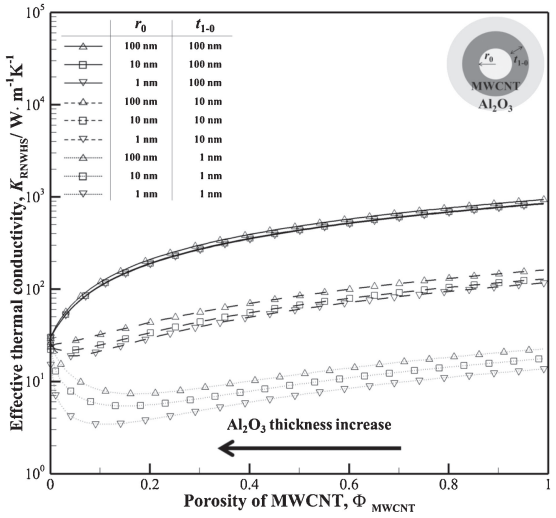


Fig. 7 Effective thermal conductivity of MWCNT/$Al_2O_3$ tubular–shell RNWHS with respect to MWCNT porosity in terms of pore radius and tubular thickness.

is affected mainly by the increase in the core radius and porosity of an MWCNT.

Figure 5(b) shows the effect of the porosity and core radius of an MWCNT on the effective thermal conductivity of the MWCNT/$Al_2O_3$ core–shell RNWHS structure. The results are similar to those of the MWCNT/$SiO_2$ case, but at core radii less than 10 nm, there are such minimum values at certain porosity, indicating that the effective thermal conductivity can be controlled by the relative ratio between the shell thickness and core radius. This is because the thermal conductivity and MFP of $Al_2O_3$ are larger than those of $SiO_2$, such that the effective thermal conductivity increases at the same porosity.

Figure 6 compares the effective thermal conductivity of core–shell nanostructures in which the MWCNT core was coated by $Al_2O_3$ and $SiO_2$. The estimated thermal conductivities were nearly the same when the core radius was above 100 nm, regardless of the change in the porosity. In addition, when the MWCNT porosity was above 0.4, there was no change in the effective thermal conductivity, regardless of shell materials and core radii. Although the MFP and thermal conductivity of $Al_2O_3$ are higher than those of $SiO_2$, the MWCNT thermal conductivity was still large. Therefore, to increase the thermal conductivity of core–shell RNWHSs, the core radius of MWCNTs should be over 100 nm or the porosity should remain above 0.4.

### 3.2 The effective thermal conductivity of tubular–shell RNWHSs

For the tubular–shell RNWHSs, additional surface scattering occurs inside the pores, resulting in different effective thermal conductivity behavior. Figure 7 shows the effective thermal conductivity of an MWCNT/$Al_2O_3$ tubular–shell RNWHS with respect to MWCNT porosity, pore radius, and tubular thickness of the MWCNT. When the MWCNT thickness was larger than 10 nm, the effective thermal conductivity increased gradually with increasing porosity of the MWCNT resulting from the decrease in $Al_2O_3$ shell thickness. This is natural because the thermal conductivity of an MWCNT is substantially higher than that of $Al_2O_3$. However, as the MWCNT thickness decreased, there existed

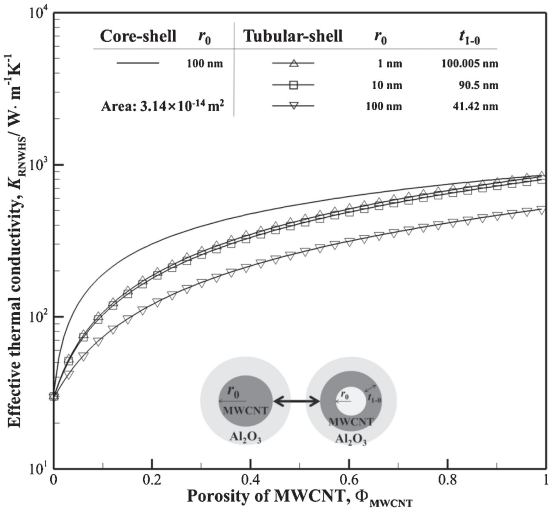


Fig. 8 Comparison of effective thermal conductivity between core–shell and tubular–shell RNWHSs of MWCNT/$Al_2O_3$ of core radius $r_0 =$ 100 nm.

a minimum effective thermal conductivity at a porosity of MWCNT. These results indicate that the effective thermal conductivity can increase by controlling the shell thickness when the MWCNT layer is approximately 1 nm thick.

There are several possible ways to increase the effective thermal conductivity of an MWCNT/$Al_2O_3$ tubular–shell structure. One way is to increase the thickness of the tubular MWCNT when the pore radius is fixed. Consequently, increasing the total radius of this structure can enhance the effective thermal conductivity.[14] It can also be enhanced by increasing the pore radius, but as observed in case of $t_{1-0} = 100$ nm, the effective thermal conductivity was rarely affected by the change of pore radius. Finally, the thermal conductivity can be increased by a decrease in $Al_2O_3$ shell thickness, which means an increase in MWCNT porosity.

Figure 8 compares the effective thermal conductivity with respect to porosity estimated for core–shell and tubular–shell RNWHS types comprising MWCNTs and $Al_2O_3$. The core radii of the core–shell types for Fig. 8 was 100 nm, and the areas was $3.14 \times 10^{-14}$ m$^2$. In both instances, the effective thermal conductivity of the core–shell type was higher than that of the tubular–shell type. These results indicate that additional energy scattering at the interface between the pores and MWCNTs may be caused by the presence of pores inside the RNWHSs. Moreover, the effective thermal conductivity increased gradually with increasing porosity.

### 3.3 The effective thermal conductivity of core–shell–shell RNWHSs

This study conducted a numerical calculation for a core–shell–shell RNWHS structure made with an MWCNT core and two coated layers, an inner layer of $Al_2O_3$ and an outer layer of W. Figure 9(a) shows the influence of the $Al_2O_3$ layer thickness on the effective thermal conductivity. The decrease in the porosity means an increase in W thickness, and for the core–shell–shell type, there are limits to the core MWCNT porosity because the $\Phi_0$ limit is $r_0^2/(r_0 + t_{1-0})^2$, at which point there is no tungsten content in the RNWHS. In

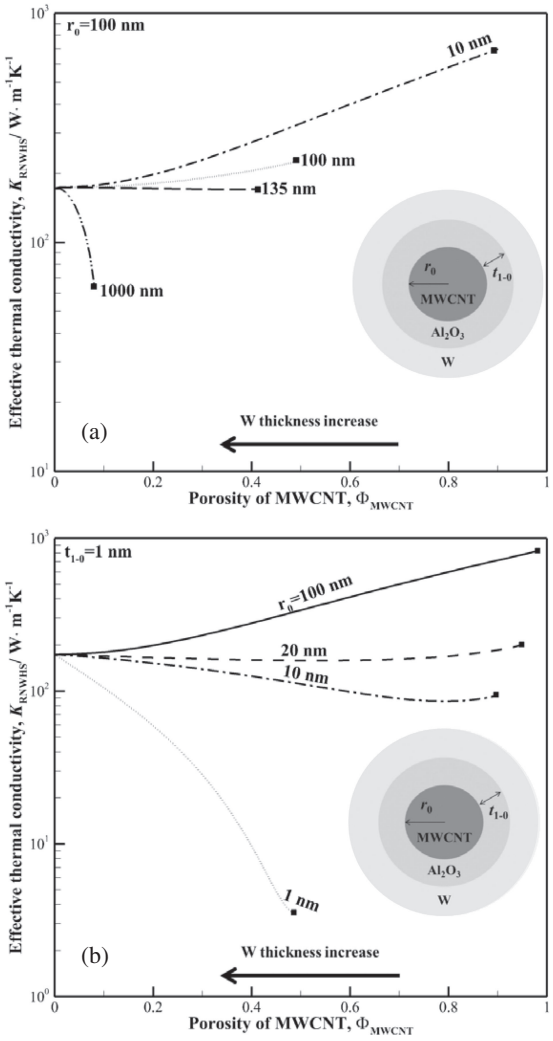


Fig. 9 Effective thermal conductivity of core–shell–shell MWCNT/$Al_2O_3$/W RNWHS with respect to MWCNT porosity at (a) fixed core radius and (b) fixed $Al_2O_3$ shell thickness.

this case, the core–shell–shell type eventually becomes just a core–shell type. Thus, zero MWCNT porosity indicates that the effective thermal conductivity of the RNWHS is the same as the bulk thermal conductivity of tungsten.

In Fig. 9(a), the thermal conductivity significantly varied with $Al_2O_3$ thickness, but when $t_{1-0}$ was smaller than 10 nm, there was rarely variation in the effective thermal conductivity, which is very similar to the results shown in Fig. 5. This result is caused by the fact that when the shell thickness of $Al_2O_3$ is equal to or smaller than the MFP (~95.1 nm), ballistic phonon transport becomes dominant and $Al_2O_3$ shell thickness does not affect the enhancement of thermal conduction.

The effective thermal conductivity increased with decreasing thickness of the tungsten shell. It is interesting to note that a rapid increase in thermal conductivity was found as the thickness of the $Al_2O_3$ shell increased to 1000 nm. This anomalous trend is attributed to occur because diffusive thermal transport takes place inside the structure. These results indicate that a relative ratio of shell thickness to core radius, which affects the interfacial scattering, is important in controlling thermal enhancement in the core–shell–shell

RNWHS. Moreover, in terms of the influence of the core radius on thermal conductivity at $t_{1-0} = 1$ nm, as depicted in Fig. 9(b), the effective thermal conductivity rapidly decreased with the increase in porosity at a very small MWCNT core radius of 1 nm, but the increase in core radius contributed to the enhancement of thermal conduction.

## 4. Conclusions

The present study conducted extensive calculations in order to model the effective thermal conductivity of RNWHSs with MWCNT cores, and the following conclusions were drawn:

(1) The effective thermal conductivity of the RNWHSs decreased by one order of magnitude below the bulk thermal conductivity of MWCNTs across the whole range of porosities because of the diffusive interfacial scattering effect rather than phonon dispersion. When the shell thickness was much thinner than the core radius, the thermal conductivity of the MWCNT core became relatively higher than that of the shell material. The effective thermal conductivity of the MWCNT/$Al_2O_3$ RNWHS was also larger than that of the MWCNT/$SiO_2$ RNWHS when the core radius was smaller than 10 nm because the bulk thermal conductivity and the MFP of $Al_2O_3$ were higher. However, the effective thermal conductivities were nearly the same when either the core radius was greater than 100 nm or the MWCNT porosity was above 0.4 because the thermal conductivity of MWCNTs is much higher than that of any other material.

(2) The increased thickness of the MWCNT in the tubular–shell RNWHS at a fixed pore radius was the key to enhancing the effective thermal conductivity of the MWCNT/$Al_2O_3$ tubular–shell structure. The effective thermal conductivity increased with increasing pore radius and with decreasing $Al_2O_3$ shell thickness. However, it was observed that the effective thermal conductivity of the core–shell RWNHS with the same cross-sectional area was higher than that of the tubular–shell RNWHS because of additional interfacial scattering at the pores inside the RNWHS. As the pore radius increased, moreover, the effective thermal conductivity significantly decreased across the whole range of porosities.

(3) For the case of the core–shell–shell RNWHS (MWCNT/$Al_2O_3$/W), when the $Al_2O_3$ thickness was less than 135 nm at a fixed core radius of 100 nm, the effective thermal conductivity increased with the increase in MWCNT porosity. When the $Al_2O_3$ thickness was 1 nm, in particular, the effective thermal conductivity rapidly decreased with the increase in porosity at an MWCNT core radius of 1 nm. However, when the $Al_2O_3$ thickness was smaller than 10 nm, the effective thermal conductivity rarely varied because the shell thickness of the $Al_2O_3$ was smaller than the MFP owing to the ballistic phonon transport effect. Therefore, to increase the thermal conductivity of RNWHSs with MWCNTs, the radius and porosity of the MWCNTs need to be greater than those of other shell materials.

## Acknowledgements

This work was supported by the National Research Foundation of Korea (NRF) grant funded by the Korea government (MSIP) (No. 2014R1A2A2A01006186). Moreover, this research was supported by the Chung-Ang University Excellent Student Scholarship in 2013.

## REFERENCES

1) G. H. Dong and Y. J. Zhu: Chem. Eng. J. **193–194** (2012) 227–233.
2) Y. T. Chong, D. Görlitz, S. Martens, M. Y. E. Yau, S. Allende, J. Bachmann and K. Nielsch: Adv. Mater. **22** (2010) 2435–2439.
3) H. Im and J. Kim: J. Mater. Sci. **47** (2012) 6025–6033.
4) C. W. Nan, Z. Shi and Y. Lin: Chem. Phys. Lett. **375** (2003) 666–669.
5) W. Tian and R. Yang: J. Appl. Phys. **101** (2007) 054320.
6) N. Hashimoto, S. Oie, H. Homma and S. Ohnuki: Mater. Trans. **55** (2014) 458–460.
7) H. Kurita, H. Kwon, M. Estili and A. Kawasaki: Mater. Trans. **52** (2011) 1960–1965.
8) P. Kim, L. Shi, A. Majumdar and P. McEuen: Phys. Rev. Lett. **87** (2001) 215502.
9) D. J. Yang, Q. Zhang, G. Chen, S. F. Yoon, J. Ahn, S. G. Wang, Q. Zhou, Q. Wang and J. Q. Li: Phys. Rev. B **66** (2002) 165440.
10) H. Im and J. Kim: Carbon **50** (2012) 5429–5440.
11) A. S. Cavanagh, C. A. Wilson, A. W. Weimer and S. M. George: Nanotechnology **20** (2009) 255602.
12) E. N. Konyushenko, J. Stejskal, M. Trchová, J. Hradil, J. Kovářová, J. Prokeš, M. Cieslar, J. Y. Hwang, K. H. Chen and I. Sapurina: Polymer **47** (2006) 5715–5723.
13) S. Yun, H. Im and J. Kim: Mater. Trans. **52** (2011) 564–567.
14) H. Im, Y. Hwang, J. H. Moon, S. H. Lee and J. Kim: Compos. Part a-APPL S. **54** (2013) 159–165.
15) Y. Zhang, S. Xiao, Q. Wang, S. Liu, Z. Qiao, Z. Chi, J. Xu and J. Economy: J. Mater. Chem. **21** (2011) 14563.
16) W. Cui, F. Du, J. Zhao, W. Zhang, Y. Yang, X. Xie and Y.-W. Mai: Carbon **49** (2011) 495–500.
17) C. F. Herrmann, F. H. Fabreguette, D. S. Finch, R. Geiss and S. M. George: Appl. Phys. Lett. **87** (2005) 123110.
18) X. Lü: Appl. Phys. Lett. **96** (2010) 243109.
19) M.-J. Huang and T.-Y. Kang: Int. J. Therm. Sci. **50** (2011) 1156–1163.
20) R. Yang, G. Chen and M. S. Dresselhaus: Nano Lett. **5** (2005) 1111–1115.
21) R. Yang, G. Chen and M. S. Dresselhaus: Phys. Rev. B **72** (2005) 125418.
22) R. Prasher: Appl. Phys. Lett. **89** (2006) 063121.
23) X. Lü: J. Appl. Phys. **106** (2009) 064305.
24) X. Lü: J. Appl. Phys. **109** (2011) 044310.
25) G. J. Hu and B. Y. Cao: Mol. Simulat. **38** (2012) 823–829.
26) H. R. Shanks, P. D. Maycock, P. H. Sidles and G. C. Danielson: Phys. Rev. **130** (1963) 1743–1748.
27) K. T. Regner, D. P. Sellan, Z. Su, C. H. Amon, A. J. H. McGaughey and J. A. Malen: Nat. Commun. **4** (2013) 1640.
28) R. G. Munro: J. Mater. Sci. **80** (1997) 1919–1928.
29) R. H. French, H. Müllejans and D. J. Jones: J. Am. Ceram. Soc. **81** (1998) 2549–2557.
30) D. A. Gryaznykh: Tech. Phys. **45** (2000) 836–839.
31) Y. D. Kim, N. L. Oh, S. T. Oh and I. Moon: Mater. Lett. **51** (2001) 420–424.